Acta Cryst. (1986). B**42**, 201-208

Charge Density in Cuprite, Cu_2O

BY R. RESTORI AND D. SCHWARZENBACH

Institut de Cristallographie, Université de Lausanne, 1015 *Lausanne, Switzerland*

(*Received* 22 *July* 1985; *accepted* 19 *December* 1985)

Abstract

Results of charge-density studies of Cu_2O have been unimpressive for years, and the agreement between different research groups has been marginal. In this work, the influence of data-reduction procedures, temperature-factor models and deformation models on the results is studied with the aim to identify robust features. Eight deformation-density refinements have been carried out with respect to data measured with Ag $K\alpha$ radiation to $(\sin\theta/\lambda)_{max} = 1{\cdot}73$ Å^{-1}. It is shown that standard Fourier methods lead to unsatisfactory results, since $\frac{3}{8}$ of the structure factors are too small to be measured. Model maps reproducibly show a density deficit along the linear O–Cu–O bond axis. This feature corresponds to the only robust variable, the population coefficient of the y_{40}-hexadecapolar function of Cu. Inclusion of anharmonic displacement parameters results in bonds with cylindrical symmetry. The maps and the interpretation in terms of an orbital-product formalism are in good agreement with modern theoretical work: Cu^{1+} ions with electron configuration $d^8(ds)^2$ in the field of O^{2-} ions form $\alpha\psi(3d_{z^2}) + \beta\psi(4s)$ hybrid orbitals, with $|\beta/\alpha| \approx 0{\cdot}7$ (2). The electric field gradient at the site of Cu cannot be computed from the X-ray data.

Introduction

The lattice complexes formed by Cu and O in the cubic ($Pn3m$) structure of the semiconductor cuprite, Cu_2O, are F and I, respectively. Cu occupies site 4(b), $\bar{3}m$, 000, $0\frac{1}{2}\frac{1}{2}$○, and O site 2(a), $\bar{4}3m$, $\frac{1}{4}\frac{1}{4}\frac{1}{4}$, $\frac{3}{4}\frac{3}{4}\frac{3}{4}$, with $a = 4{\cdot}627$ (2) Å. These f.c.c. and b.c.c. substructures interpenetrate in such a way that O is tetrahedrally coordinated by four Cu, and Cu linearly by two O. The Cu–O distance is 1·848 Å, whereas the distances between like atoms are much longer, 3·017 Å for Cu–Cu and 3·695 Å for O–O. The structure is in fact *uniquely* defined by requiring a linear coordination of close-packed Cu: the stoichiometry then requires the occupation of tetrahedral sites by O; any other stacking variant but the cubic one, or occupation of tetrahedral sites other than those of the actual structure leads to O–Cu–O angles different from 180°. The structure with the exact 2:1 stoichiometry is therefore not expected to be disordered. Also interesting are the two kinds of inequivalent Cu–Cu contacts of equal length. The structure can be thought of as formed by two identical interpenetrating substructures (Wells, 1975) composed of Cu, arranged as in the cubic Laves phase $MgCu_2$, and O, arranged in a diamond-type network. These substructures are independent in the sense that there is no path leading from the one to the other *via* contiguous Cu–O vectors. Cu–Cu contacts within one substructure (edges of occupied tetrahedra) have $mm2$ symmetry, those between the substructures 222 symmetry. This degeneracy of the contact lengths cannot be lifted with a simple structural deformation. It therefore represents a geometrical constraint and is hardly indicative of a particular interaction between Cu atoms.

A qualitative model of the linear O–Cu–O bond, which is based on ligand-field theory and agrees with the diamagnetic and semiconducting properties of Cu_2O, has been proposed by Orgel (1958). This model assumes an essentially ionic compound in which Cu^{1+} forms a d^8 plus doubly occupied $3d_{z^2}$-$4s$ hybrid state instead of the spherically symmetric d^{10} state. This removes electrons from the bond axis z, spreads them in the diffuse $4s$ orbital, and permits the O^{2-} ions to approach much closer than the sum of the ionic radii, 2·3 Å. The hybrid orbital $\alpha\psi(d_{z^2}) + \beta\psi(4s)$, of symmetry a_{1g}, is more effective in the charge depletion at distances from Cu^{1+} larger than about 0·8 Å if β/α is negative. Recent theoretical calculations agree with this bonding scheme. The principal feature of the difference density map obtained by Marksteiner, Blaha & Schwarz (1986) with LAPW band structure calculations indeed resembles a cylindrically symmetric unoccupied d_{z^2} orbital $\Delta\varrho \approx -|\psi(d_{z^2})|^2$ centered on Cu. Nagel (1985) obtained a very similar result with an MSX_α cluster calculation although he included only atoms of one of the two interpenetrating substructures, and thus only Cu–Cu contacts with $mm2$ symmetry. The Cu–Cu interactions do not, therefore, seem to be important for the stability of the structure. The hybridization was computed to be $\beta/\alpha \approx -\frac{1}{2}$.

The electric field gradient tensor at the site of Cu has axial symmetry and is thus completely described by one component, $\nabla E_{zz} = -(\partial^2 V/\partial z^2)$ (z along $\bar{3}$, V = electrostatic potential). The quadrupole coupling

0108-7681/86/030201-08$01.50

constants $|eQ\nabla E_{zz}/h|$ for ^{63}Cu and ^{65}Cu (eQ = nuclear quadrupole moment, h = Planck's constant) have been measured with nuclear quadrupole resonance spectroscopy (NQR) by Krüger & Meyer-Berkhout (1952). Taking $Q = -16\ fm^2$ and $-15\ fm^2$ for ^{63}Cu and ^{65}Cu, respectively (*Handbook of Chemistry and Physics*, 1980), one obtains one of the largest field gradients known, $|\nabla E_{zz}| = 134\times10^{20}\ V\ m^{-2}$. On the basis of an ionic point-charge model, ∇E_{zz} is computed to be positive (Hafner & Nagel, 1983), whereas the MSX_α cluster calculation (Nagel, 1985) gave a satisfactory agreement with the experimental quadrupole coupling constant, and a negative sign.

The present research on Cu_2O has been prompted by our interest in the calculation of electric field gradients from structure factors and the use of experimentally measured field gradients for the determination of electron-density distributions (Lewis, Schwarzenbach & Flack, 1982, and references cited therein). During the course of the work, the more basic question of the feasibility of an electron-density study of a heavy-atom structure like Cu_2O by X-ray diffraction methods became more prominent.

Experimental

The structure factors of Cu_2O belong to the following classes according to the even (e) or odd (o) parity of the indices hkl:

$$F_{hkl} = M(\mathrm{Cu}) \pm M(\mathrm{O}) + H_1(\mathrm{Cu}) \pm H(\mathrm{O}) \qquad eee\text{ -strong}$$
$$M(\mathrm{Cu}) \quad + H_1(\mathrm{Cu}) \pm \mathrm{Oct(O)} \qquad ooo\text{ -strong}$$
$$\pm M(\mathrm{O}) + Q(\mathrm{Cu}) + H_2(\mathrm{Cu}) \pm H(\mathrm{O}) \qquad ooe\text{-medium}$$
$$Q(\mathrm{Cu}) + H_2(\mathrm{Cu}) \pm \mathrm{Oct(O)} \qquad eeo\text{-very weak}$$

The notation symbolizes scattering factors of atom-centered multipoles (Kurki-Suonio, 1977): M = monopole, including the free-atom scattering factors $4f(\mathrm{Cu})$ and $2f(\mathrm{O})$; Q = quadrupole y_{20}, including the anisotropic temperature factor of Cu; H_1, H_2, H = hexadecapoles $a_1y_{40} + b_1y_{43+}$, $a_2y_{40} - b_2y_{43+}$ and $K_4 = y_{40} + y_{44+}/168$, respectively; Oct = octopole $K_3 = y_{32-}$.

Spherical crystals of Cu_2O were prepared with a crystal grinder (Enraf–Nonius) from a natural specimen of imprecisely specified origin (eastern USA). A sphere of diameter 0·105 mm was chosen for data collection at 100 K on an Enraf–Nonius CAD-4 diffractometer using LiF-monochromated Ag $K\alpha$ radiation ($\lambda\alpha_1 = 0{\cdot}55941$ Å), a nitrogen-gas-flow cooling device and the 2θ–ω scan technique. The temperature fluctuations near the nozzle inside the Dewar tube were less than 1 K. The 002 reflection of LiF was used instead of the standard graphite monochromator because its larger reflection angle of $2\theta = 16{\cdot}015°$ permitted a much more satisfactory alignment. In addition, the backgrounds of the Cu_2O reflections were lower when using LiF, and this should be advantageous for the measurement of the weak *eeo* reflections. On the other hand, the splitting of the α_1–α_2 doublet at the site of the Cu_2O crystal was of the same order as the diameter of the sphere, making the use of the LiF monochromator undesirable except for very well centered spheres. The scan angle ω was $(1{\cdot}5 + 0{\cdot}45\tan\theta)°$; the counter aperture width was 1·325° vertical and 1·987° horizontal. All symmetry-equivalent reflections were measured as detailed in Table 1. Backgrounds were estimated in two ways: (a) by using the CAD-4 diffractometer program which assumes the first and last sixths of the scan to be background; (b) by applying the minimum $\sigma(I)/I$ criterion (Blessing, Coppens & Becker, 1972). Three intensity-control reflections at $\theta = 5{\cdot}3$, 18·7 and 24·5° were measured every 3 h. The variance of an intensity was computed according to $\sigma^2(I) = \sigma^2(\text{counting statistics}) + (KI)^2$ where $K \approx 0{\cdot}002$ was obtained from this formula by analyzing the fluctuations of the control reflections about their mean values. The 1974 ψ-scan data, collected for $-60° < \psi < 60°$ in steps of 20°, showed only small fluctuations, and anisotropic extinction effects were thus judged to be unimportant. Absorption factors ranged from 2·468 to 2·948 ($\mu = 14{\cdot}364\ mm^{-1}$, $\mu R = 0{\cdot}754$). Absorption weighted mean path lengths were taken from Flack & Vincent (1978). The thermal diffuse scattering (TDS) correction $I_o = \alpha I$ (Bragg) was evaluated with a program based on Stevens (1974), using the elastic stiffness constants at 100 K: $c_{11} = 11{\cdot}93$, $c_{12} = 10{\cdot}35$, $c_{44} = 1{\cdot}14\times10^{10}\ Nm^{-2}$ (Hallberg & Hanson, 1970). The very low shear modulus c_{44} permits the propagation of high-amplitude transverse waves, and α therefore reaches values more typical of organic compounds. On the other hand, the correction is nearly isotropic since $\frac{1}{2}(c_{11} - c_{22}) = 0{\cdot}79 \approx c_{44}$. It corresponds approximately to an artificial temperature factor $1/\alpha \approx \exp[-0{\cdot}12(\sin\theta/\lambda)^2]$ at 100 K with $(1/\alpha)_{\min} = 0{\cdot}70$. Note that at room temperature it is three times larger. Unweighted mean values $\bar{I}$ of n symmetry-equivalent reflections I_i were computed from 4945 intensities omitting the ψ-scan data. For the variance of $\bar{I}$, the larger of the two quantities $\sigma_1^2(\bar{I}) = \sum\sigma^2(I_i)/n^2$ and $\sigma_2^2(\bar{I}) = \sum(I_i - \bar{I})^2/n(n-1)$ was chosen. Generally, σ_1 and σ_2 agree well, the largest differences approaching 20% for some low-order reflections. Internal R values are 0·0263 and 0·0252 for background corrections (a) and (b) respectively, which corresponds to $\sigma(\bar{I})/\bar{I}$ values ranging from 0·01 to 0·03 for strong and weak reflections respectively, the highest orders being somewhat less accurate.

The number of independent data is 171, 163 with $\bar{I} > 3\sigma(\bar{I})$. None of the *eeo* reflection intensities are unambiguously observed. For the three reflections 221, 223 and 421 with θ between 0 and 18°, $\bar{I}/\sigma(\bar{I})$

Table 1. *Data collection*

Parity of *hkl*	θ(°)	$(\sin\theta/\lambda)_{max}$ (Å^{-1})	Scan speed (° min^{-1})	*R*(internal)* *a*	*b*
eee,ooo	0–35	1·02	2·50	0·0249	0·0243
eee, ooo	35–75	1·73	0·67		
ooe, oeo, eoo	0–23	0·70	0·67	0·1038	0·0767
ooe, oeo, eoo	23–43	1·22	0·17		
eeo, eoe, oee	0–18	0·55	0·033		
ψ scans *eee, ooo*	0–35	1·02	2·50	0·0197	0·0197

* For *a*, *b* see text.

is 1·4, 0·0 and 3·3 respectively. Measurements at higher angles did not indicate any other *eeo* reflections to be observable. As to the *ooe* reflections, $\bar{I}/\sigma(\bar{I})$ values fall below 3 at $\theta > 43°$.*

All data-reduction calculations were carried out with a local version of the *XRAY* system (1972). The free-atom scattering factors in analytical form and the dispersion corrections were taken from *International Tables for X-ray Crystallography* (1974).

Charge-density refinement

Our charge-density refinement program *LSEXP* presently provides the following options, in addition to the standard procrystal model defined by positional and harmonic displacement parameters, scale factor and secondary-extinction parameters (Becker & Coppens, 1974, 1975):

(*a*) 3rd- and 4th-order anharmonic displacement parameters are represented by the Gram–Charlier series expansion formalism (Johnson & Levy, 1974).

(*b*) Aspherical atoms are represented by a sum of up to 35 multipolar deformation functions

$$\varrho_{nlm\pm} = P_{nlm\pm}\varrho_n(r)C_{lm\pm}y_{lm\pm} \qquad (1)$$

(Stewart, 1976) which are exactly equivalent to the 35 deformation functions of Hirshfeld (1977): three monopoles $l=0$, $n=0,2,4$; two dipoles $l=1$, $n=1,3$; two quadrupoles $l=2$, $n=2,4$; one octopole $l=3$, $n=3$; and one hexadecapole $l=4$, $n=4$. $C_{lm\pm} = 1/\int|y_{lm\pm}|\mathrm{d}\Omega$ is a normalization constant, $P_{nlm\pm}$ is a refineable population parameter.

(*c*) As is usual, the radial functions may be represented by $\varrho_n = N_n r^n \exp(-\alpha r)$, where N_n is a normalization factor such that $\int r^2\varrho_n(r)\,\mathrm{d}r = 1$ and α is a refineable parameter. For the monopolar terms $l=m=0$, the κ formalism may be used (Coppens, Guru Row, Leung, Stevens, Becker & Yang, 1979). Moreover, in what we call a *mixed basis*, the functions for $n=l$ may be represented by the Lorentzians $\varrho_n = N'_n x^n/(1+x^2)^{n+2}$, $x=r/\beta$, while for $n\neq l$, the exponential functions are retained, and α and β are independently refineable. The Fourier transforms of exponentials are Lorentzians and *vice versa*. If the former are diffuse, then the latter peak quite sharply. Gaussians are intermediate between these functions.

Models with only a few refineable parameters usually show good numerical stability, but they also may have some unrealistic features. Flexible models, on the other hand, often present numerical problems due to high correlations between refined parameters. Thus, by not including anharmonic displacement terms, rather small e.s.d.'s of electron-density parameters may be obtained. Much larger e.s.d.'s are generally obtained when anharmonic terms are included, since thermal-motion and bonding-density effects cannot easily be distinguished on the basis of X-ray data. This observation should not lead to a more restricted model, but rather to a more cautious interpretation of the results. In the case of completely correlated variables, the data give no information on their individual values. One of these variables may then be held fixed at an arbitrary value with no loss of quality of the parametrization of the data.

The 12 multipole functions used in the present work are y_{00} ($n=0,2,4$), y_{20} ($n=2,4$), y_{40} and y_{43+} ($n=4$) for Cu, and $K_0 = y_{00}$ ($n=0,2,4$), $K_3 = y_{32-}$ ($n=3$) and $K_4 = y_{40} + y_{44+}/168$ ($n=4$) for O. The local coordinate system for Cu is z along the threefold axis [111] and y perpendicular to the mirror plane of $\bar{3}m$ [$\bar{1}$10]; for O it corresponds to the cubic lattice base. All refinements were with respect to $|F|^2$. The general isotropic-extinction correction included two variables, G for the mosaic spread and R for the domain size. Lowest reliability indices for the procrystal model were obtained with a Lorentzian mosaic distribution. The smallest extinction factor y_{min} ($F_o = yF_{corr}$) was 0·86. Refinement of the population parameters of the atoms in the procrystal model did not indicate either a deviation from the ideal stoichiometry, or a contaminating contribution of $\lambda/2$ radiation to the *ooe* reflections. Eight full-matrix deformation-density refinements (Table 2) were carried out, *viz* using structure amplitudes obtained with the standard background correction or with the minimum $\sigma(I)/I$ criterion (N or L), including only harmonic displacement parameters or seven additional 3rd- and 4th-order anharmonic parameters (H or G), assuming the exponential basis or the mixed basis (E or M). In each case, 100 to 200 cycles with shift damping factors of 0·1 to 0·3 were sufficient to reach convergence at (full shift/variable) values smaller than 10^{-4}. An additional 100 cycles did not change the results. In some refinements, one or several of the electron density variables α(Cu), α(O), P_{332-}(O) did not reach stable values, but continued to change while reliability indices were increasing. They were fixed at the values they had reached when the goodness of fit (GOF) started to increase, and refinement of the other parameters was then con-

* Lists of structure factors and deformation parameters have been deposited with the British Library Lending Division as Supplementary Publication No. SUP 42674 (4 pp.). Copies may be obtained through The Executive Secretary, International Union of Crystallography, 5 Abbey Square, Chester CH1 2HU, England.

Table 2. *Temperature, reliability and scale factors*

Definitions: $GOF(|F^2|) = [\sum w(|F_o|^2 - |F_c|^2)^2/(n-m)]^{1/2}$; n = number of observations, m = number of variables; $R(|F|) = \sum ||F_o| - |F_c|| / \sum |F_o|$; $wR(|F|^2) = [\sum w(|F_o|^2 - |F_c|^2)^2 / \sum w|F_o|^4]^{1/2} \approx 2wR(|F|)$. The scale factor is defined by $F_o = \text{scale} \times y \times F_{corr} = \text{scale} \times F_c$, y being the extinction correction. The temperature-factor expression is $\exp(-2\pi^2 a^{-2} \sum U_{ij} h_i h_j)$; e.s.d's are given in parentheses. ∇E_{zz} is the electric-field gradient along the Cu-O bond at the site of Cu in 10^{20} V m^{-2}, e.s.d ≈ 300. N = standard background treatment, L = minimum $\sigma(I)/I$, H = harmonic displacement parameters, G = Gram-Charlier expansion, E = exponential basis, M = mixed basis.

	Pro-crystal, *N*	*NHE*	*NHM*	*NGE*	*NGM*	*LHE*	*LHM*	*LGE*	*LGM*
$10^5 U_{11}$ (Cu)	765 (2)	779 (5)	781 (6)	718 (22)	757 (50)	774 (7)	786 (6)	719 (25)	771 (33)
$10^5 U_{12}$ (Cu)	−37 (2)	−54 (16)	−34 (6)	11 (29)	33 (32)	−65 (14)	−88 (25)	12 (34)	33 (33)
$10^5 U$(O)	836 (9)	848 (22)	866 (15)	980 (746)	883 (200)	811 (18)	836 (17)	1024 (14)	962 (82)
GOF($\|F\|^2$)	1·14	0·966	0·943	0·925	0·916	1·106	1·105	1·103	1·079
$R(\|F\|)$	0·01028	0·00873	0·00813	0·00837	0·00798	0·00878	0·00879	0·00863	0·00825
$wR(\|F\|^2)$	0·01482	0·01107	0·01076	0·01028	0·01009	0·01207	0·01212	0·01170	0·01140
$n-m$	145	131	130	124	122	127	128	121	120
Scale	19·96 (3)	20·29 (16)	20·52 (22)	19·85 (17)	20·22 (99)	19·19 (27)	19·67 (20)	19·65 (20)	20·43 (65)
∇E_{zz}	−1·18	999	−31	−99	−440	1415	4611	204	−537
Fixed parameters		—	α(O)	—	—	—	α(O), α(Cu) P_{332-}(O)	α(O)	α(O), P_{332-}(O)

tinued. The introduction of anharmonic displacement parameters did not result in numerical problems or difficulties of convergence. At no stage was the physical reasonableness of the resulting values of the variables tested, *i.e.* the different models serve only to parametrize the experimental data. Thus, the scale factor varies by 6·7%, and we see no basis for preferring one value rather than another.

Out of the 22 reflections with $\sin\theta/\lambda > 1{\cdot}6$ Å^{-1}, 14 showed abnormally large $w^{1/2}(|F_o|^2 - |F_c|^2)$ values in *all* refinements, *e.g.* −10 and 14 for 10,8,6 and 13,5,1, respectively. Their individual intensity profiles were re-examined and indeed showed some anomalies, *viz* abnormally high and/or unequal background to the left and right of the peak, the physical reasons of which remain unexplained. These reflections, as well as 321, which also showed unequal left and right backgrounds, were given zero weight.

The relatively small differences between final reliability factors (Table 2) of the procrystal and charge-density refinements show clearly the smallness of the effect of the bonding electrons on the X-ray intensities, and the overwhelming domination of the core electron density of Cu. Studies of heavy-atom compounds like Cu_2O thus require more accurate structure factors than studies of organic light-atom compounds. But, at the same time, the experiments are far more difficult to perform, mainly due to absorption and extinction effects.

Results

(*a*) *Difference Fourier maps*

Conventional X-X difference maps based on the procrystal refinement, and X-N maps at room and at low temperatures (Mullen & Fischer, 1981; Eichhorn, Spilker & Fischer, 1984) led to diverse, ambiguous interpretations. They had, however, one property in common: important features around Cu at 000 were repeated as mirror images around the empty site $00\frac{1}{2}$. This effect is akin to a pseudo-translation of the f.c.c. Cu atoms by $[\frac{1}{2}\frac{1}{2}\frac{1}{2}]$. For the features near O, an analogous pseudo-translation $[\frac{1}{2}\frac{1}{2}0]$ is observed. As an example equivalent to an actual X-X map, Fig. 1(*a*) shows the results of a Fourier summation of the static structure factors calculated with the deformation functions of refinement *NGE*, but using only the terms corresponding to the 171 measured reflections (Table 1). The pseudo-translation effect is seen to be due to the omission of the very large number of pseudo-extinct *eeo* reflections, which represent $\frac{3}{8}$ of reciprocal space, but which had intensities too small to be measured. Similar results are obtained at resolutions as low as $(\sin\theta/\lambda)_{max} = 0{\cdot}80$ Å^{-1}. By including in the Fourier summation also the *calculated* structure factors (refinement *NGE*) of all 97 *eeo* and 79 *ooe* reflections which were not measured, the pseudo-translations disappear (Fig. 1*b*). None of these calculated intensities was strong enough to be observable with our equipment, but their combined contribution is non-negligible.

Even though by hindsight the X-X maps showed some essential features of the final maps (Figs. 2*a*-2*d*), they are inappropriate for an electron-density study, and results can be obtained only by using deformation models.

(*b*) *Model maps*

Four model deformation-density maps (*N*..) at infinite resolution, obtained by summation of the deformation functions in direct space, are shown in Figs. 2(*a*)-2(*d*). Standard deviations have been estimated by summing the variances and covariances of the deformation parameters (Hirshfeld, 1977). The corresponding maps obtained with the minimal $\sigma(I)/I$ data (*L*..) differ mainly near the centers of the atoms, and the differences are described in the figure captions. The only significant features con-

sistently seen on all maps are near Cu, those near O being quite variable. The most obvious consistent feature is a trough of negative density along the O–Cu–O bond axis. Off this axis, lobes of positive density appear near Cu. In the maps obtained with harmonic displacement parameters (*.H.*), the density distribution is skewed, whereas the use of anharmonic terms (*.G.*) leads to approximate *mm* symmetry. Since the bond axis has symmetry $\bar{3}m$, the plane $(11\bar{2})$ perpendicular to the plane $(1\bar{1}0)$ represented in Fig. 2 must show *mm* symmetry. The bond axis of the *.G.* maps is thus approximately cylindrical, ∞/mmm. In fact, as shown below, the deviation from cylindrical symmetry is given by the population coefficient P_{443+} of the y_{43+} function, which is very nearly zero for the *.G.* refinements (Table 3). The probability density functions (p.d.f.) of the anharmonic atomic displacements (Johnson & Levy, 1974) obtained with the *.G.* refinements are in agreement with intuition. The cylindrically symmetric part of the p.d.f. of Cu is very similar to the harmonic p.d.f. of the *.H.* refinements, the thermal motion being more important perpendicular than parallel to the Cu–O bond. The non-cylindrical component corresponds closely to the non-cylindrical density features of refinements *.H.*, and represents an increased thermal motion directed along ±[001] towards the centers of the octahedral voids of the f.c.c. packing of Cu. Deformation-density features and anharmonic terms for O are at most of the order of 1 e.s.d., and are thus insignificant. Still, the harmonic and anharmonic p.d.f.'s of O are quite similar, the latter showing weak lobes directed towards the faces of the Cu coordination polyhedron.

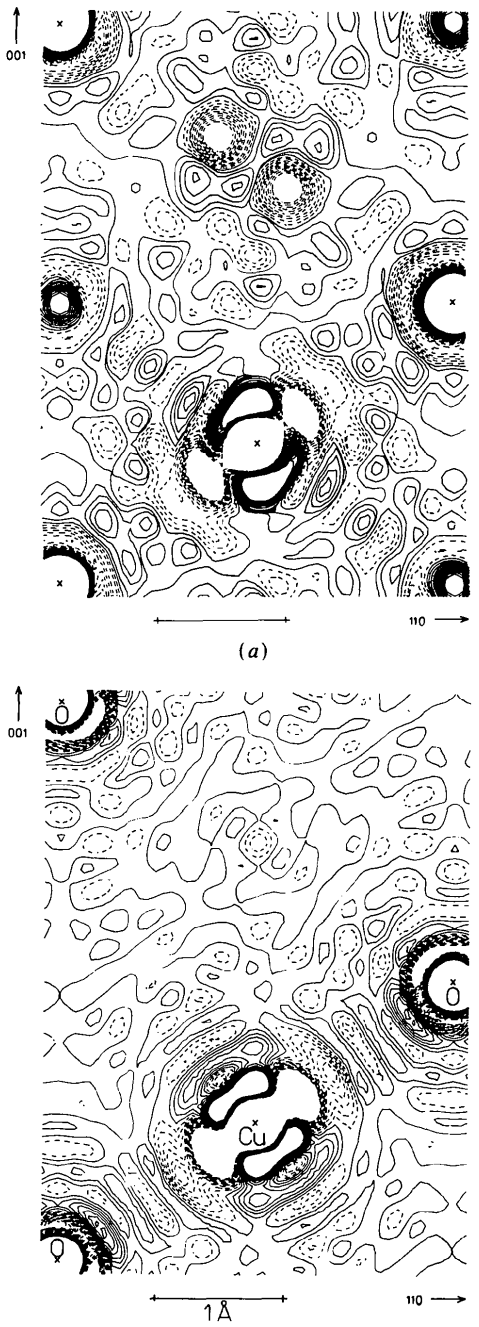

Fig. 1. Static model deformation maps of Cu_2O in the plane $(1\bar{1}0)$ obtained by Fourier summations of the structure factors calculated with the deformation functions of refinement *NGE*. Contours drawn between ±0·5 eÅ^{-3}, interval 0·05 eÅ^{-3}, negative contours broken. (*a*) Includes only structure factors of the measured reflections (Table 1). (*b*) Includes all structure factors.

The two very similar maps *NGE* and *LGE* are also similar to the theoretical results of Marksteiner, Blaha & Schwarz (1986) and of Nagel (1985). As mentioned above, the Cu–O bonds of these authors are cylindrically symmetric and suggest the removal of electrons from the d_{z^2} orbital. Even though the eight refinements do not lead to very different reliability indices, we prefer refinement *NGE* (Fig. 2*c*) for the following reasons:

(1) The anharmonic displacement parameters of *.G.* lead to better agreement with theory, and an enhanced thermal motion of Cu towards the largest unoccupied voids of the structure. This appears to be more convincing than a polarization of the electron density of Cu towards distant neighbors.*

(2) The *L..* refinements were generally less stable and require certain electron-density parameters to be held constant (Table 2). The influence of the background correction on the results has been described by van der Wal, de Boer & Vos (1979). The minimal $\sigma(I)/I$ criterion may introduce a bias particularly in the weak intensities, even though the agreement between measurements of symmetry-equivalent reflections is improved (Table 1).

(3) The mixed basis *..M* is at least as efficient for the parametrization of the X-ray data as the exponential basis *..E*, but it does not seem to offer any particular advantage.

* We are aware of two research groups presently engaged in the interpretation of neutron data of Cu_2O.

(c) *Field gradient*

The field gradient ∇E_{zz} along the bond axis has been computed by Fourier series (Schwarzenbach & Ngo Thong, 1979) and by summation in direct space. Table 2 shows the results to be very model dependent. Not even the sign of ∇E_{zz} can be predicted, the good agreement of the result of *NGE* with experiment and theory being probably fortuitous. As could therefore be expected, imposing the experimental value of ∇E_{zz} assuming a positive or negative sign as a constraint on the refinement (Schwarzenbach & Ngo Thong, 1979) hardly modifies the results, except that the maps tend to become somewhat more symmetrical in those

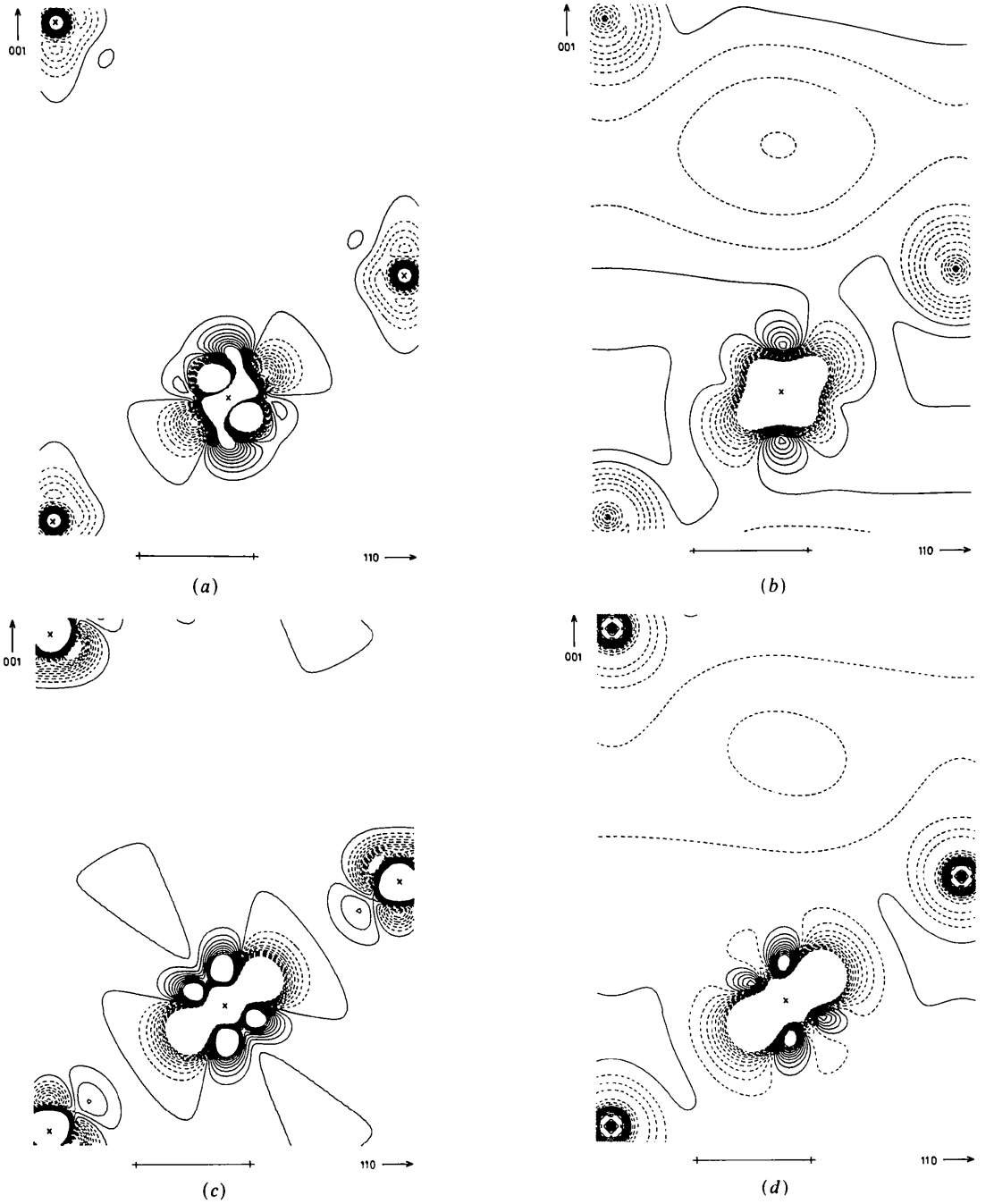

Fig. 2. Static model deformation maps at infinite resolution in the plane $(1\bar{1}0)$, refinements (*N..*). Contours drawn between ± 1 eÅ^{-3}, interval 0·1 eÅ^{-3}, negative contours broken. Features near Cu reach 3 to 4 e.s.d.'s, near O they are of the order of 1 e.s.d. On the bond axis, e.s.d.'s reach 0·1 eÅ^{-3} at 0·7 Å and 1·0 eÅ^{-3} at 0·4 Å from Cu; corresponding distances through the positive lobes are 0·6 and 0·3 Å, respectively. (*a*) Refinement *NHE*; *LHE* resembles (*b*). (*b*) Refinement *NHM*; *LHM* shows higher density at Cu and O. (*c*) Refinement *NGE*; *LGE* is in excellent agreement. (*d*) Refinement *NGM*; *LGM* shows lower densities near Cu and O.

Table 3. *Multipole populations of* Cu, *and the hybridization x*

Standard deviations in parentheses have been computed with the variances and covariances obtained from least squares.

Refinement	P_{00}	P_{20}	P_{440}	P_{443+}	P_{440}/P_{20}	$\|x\|$
NHE	0·02 (0·04)	0·3 (3)	−0·26 (6)	−0·15 (4)	−1·0 (1·2)	0·47 (6)
NHM	2·3 (4·9)	−0·3 (2)	−0·30 (6)	−0·18 (5)	1·2 (9)	0·50 (6)
NGE	0·08 (0·04)	−0·5 (3)	−0·50 (14)	−0·06 (8)	1·0 (8)	0·71 (15)
NGM	4·1 (5·6)	−1·0 (4)	−0·57 (16)	−0·09 (9)	0·6 (3)	0·79 (19)
LHE	−1·2 (0·4)	0·5 (3)	−0·33 (5)	−0·10 (5)	−0·7 (5)	0·54 (5)
LHM	−0·8 (1·2)	1·2 (6)	−0·32 (6)	−0·13 (5)	−0·3 (2)	0·53 (6)
LGE	0·14 (0·05)	−0·4 (4)	−0·49 (12)	−0·04 (8)	1·3 (1·4)	0·71 (13)
LGM	5·0 (2·5)	−1·0 (4)	−0·64 (19)	−0·04 (9)	0·6 (3)	0·88 (24)

cases where the unconstrained value of ∇E_{zz} is computed to be very large. We have to conclude that the field gradient at the site of an atom as heavy as Cu is nearly useless for an electron-density determination. Constraining it to a small value may give a marginal advantage.

Discussion in terms of orbital occupancies

Following Holladay, Leung & Coppens (1983), *d*-orbital occupancies of transition-metal atoms may be calculated from electron-density multipole parameters. Their theory supposes the multipole functions centered on the metal atom to be equivalent to the products between the metal *d* orbitals, *i.e.* the metal atom is treated as an isolated entity. The 15 products between the (normalized) *d* functions $\psi_i = \psi_{2m\pm} = R_{3d}(r)y_{2m\pm}$ (R_{3d} = radial part common to all *d* functions) result in 15 equations for 1 monopole, 5 quadrupole and 9 hexacadecapole density functions

$$\varrho_{\rm val}(\text{metal}) = \sum_i^5 \sum_j^5 A_{i,j}\psi_i\psi_j \approx \sum_{l=0,2,4} \sum_{m=-l}^{l} \left\{\sum_n \varrho_{nlm\pm}\right\} + d\text{-electron density of procrystal atom,} \quad (2)$$

where $\varrho_{nlm\pm}$ is defined in (1) and $A_{i,j}$ is the population of the orbital product. We assume in the following the existence of Cu^{1+} ions with 10 valence electrons, and use in addition to the five $3d$ orbitals also the $4s$ orbital. In the case of symmetry $\bar{3}m$ (using the same coordinate system as described for the density-functions, *z* being the bond axis), we obtain the symmetry species $a_{1g}(\psi_{z^2})$, $a'_{1g}(\psi_s)$, $e_g(\psi_{xz}, \psi_{yz})$ and $e'_g(\psi_{x^2-y^2}, \psi_{xy})$, where *s*, z^2, *xz*, *yz*, x^2-y^2, *xy* are equivalent to the indices $lm = 00, 20, 21+, 21-, 22+, 22-$, respectively. In the case of cylindrical symmetry ∞/mmm, the e_g and e'_g orbitals belong to different species π_g and δ_g, and then do not mix. Products of non-mixing orbitals do not contain the holosymmetric representation and do not result in density functions. We thus obtain for $\bar{3}m$:

$$\begin{aligned}\varrho_{\rm val}(Cu^{1+}) = {} & A_{z^2}\psi_{z^2}^2 + A_s\psi_s^2 + 2A_{z^2,s}\psi_{z^2}\psi_s \\ & + \tfrac{1}{2}A_{eg}[\psi_{xz}^2 + \psi_{yz}^2] \\ & + \tfrac{1}{2}A_{e'g}[\psi_{x^2-y^2}^2 + \psi_{xy}^2] \\ & + A_{eg,e'g}[\psi_{xz}\psi_{x^2-y^2} - \psi_{yz}\psi_{xy}], \end{aligned} \quad (3)$$

A_{z^2} meaning A_{z^2,z^2}, *etc.* Since Cu_2O is a diamagnetic semiconductor, we assume the two a_{1g} orbitals to form a hybrid

$$\psi_{ag} = \frac{1}{\sqrt{1+x^2}}\{\psi_{z^2} + x.\psi_s\}. \quad (4)$$

With population A_{ag} of ψ_{ag}^2 one obtains

$$A_{z^2} = A_{ag}/(1+x^2); \qquad A_s = A_{ag}x^2/(1+x^2);$$
$$A_{z^2,s} = A_{ag}x/(1+x^2). \quad (5)$$

Developing the orbital products into spherical harmonics as in Holladay *et al.* (1983),* we obtain using (1) and (2):

$$\begin{aligned}\varrho_{\rm val}(Cu^{1+}) = {} & \{R_{3d}^2(A_{z^2} + A_{eg} + A_{e'g}) + R_{4s}^2A_s\}D_{00} \\ & + \{0{\cdot}550\ R_{3d}^2(A_{z^2} + \tfrac{1}{2}A_{eg} - A_{e'g}) \\ & + 1{\cdot}721\ R_{3d}R_{4s}A_{z^2,s}\}D_{20} \\ & + R_{3d}^2\{0{\cdot}737\ A_{z^2} - 0{\cdot}941\ A_{eg} \\ & + 0{\cdot}123\ A_{e'g}\}D_{40} \\ & + R_{3d}^2\{0{\cdot}955\ A_{eg,e'g}\}D_{43+} \\ \approx {} & \varrho_{\rm val}(\text{free Cu}) \\ & + (P_{000}\varrho_0 + P_{200}\varrho_2 + P_{400}\varrho_4)D_{00} \\ & + (P_{220}\varrho_2 + P_{420}\varrho_4)D_{20} \\ & + P_{440}\varrho_4D_{40} + P_{443+}\varrho_4D_{43+}. \end{aligned} \quad (6)$$

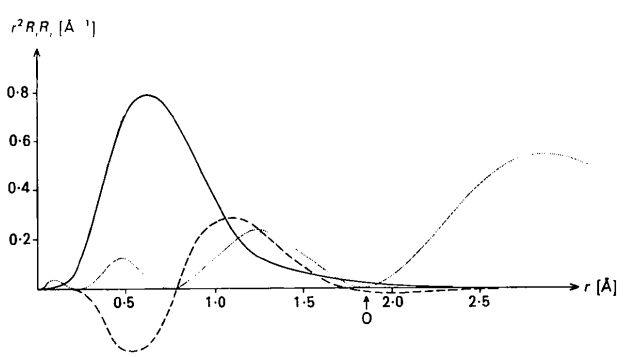

Fig. 3. Products of hydrogen-like radial wavefunctions of Cu, $r^2R_{3d}^2$ (full line), $r^2R_{4s}^2$ (dotted line) and $r^2R_{3d}R_{4s}$ (broken line).

* In contrast to this paper, our labelling of the spherical harmonics agrees with Kurki-Suonio (1977), and the density functions are normalized to $\int |D_{lm\pm}|\, d\Omega = 1$.

$D_{lm\pm} = C_{lm\pm} y_{lm\pm}$ is the normalized angular part of the density function (1). Evidently, the functions $\varrho_n(r)$ approximate the products of R_{3d} and R_{4s} only imperfectly. In order to guess the spatial extent of the latter, we have represented R_{3d} and R_{4s} with hydrogen-like radial wavefunctions based on associated Laguerre polynomials; effective atomic charges used were 7·85e for $3d$ and 4·55e for $4s$ (Atkins, 1983). Fig. 3 shows that R_{3d}^2 will probably be parametrized mainly by the density functions of Cu, R_{4s}^2 by those of O, and $R_{3d}R_{4s}$ by both. Integrating (6) over the spatial extent of the ϱ_n functions and introducing (5) then gives

$$\begin{aligned} A_{ag}/(1+x^2) + A_{eg} + A_{e'g} &\approx 11 + P_{000} + P_{200} + P_{400} \\ &= 11 + P_{00} \\ 0{\cdot}550\{A_{ag}/(1+x^2) + \tfrac{1}{2}A_{eg} - A_{e'g} + hA_{ag}x/(1+x^2)\} & \\ \approx P_{220} + P_{420} &= P_{20} \qquad (7) \\ 0{\cdot}737\, A_{ag}/(1+x^2) - 0{\cdot}491\, A_{eg} + 0{\cdot}123\, A_{e'g} &\approx P_{440} \\ 0{\cdot}955\, A_{eg,e'g} &\approx P_{443+} \\ h = 3{\cdot}130 \int_{Cu} r^2 R_{3d} R_{4s}\, dr. & \end{aligned}$$

These equations contain, of course, too many unknowns. Moreover, monopole populations are generally difficult to determine: Table 3 shows the extreme model dependence of P_{00}, due essentially to an ill-defined partitioning of the electron density between the atoms. Consistent with the physical properties of Cu_2O, we assume therefore an electronic configuration $d^8(ds)^2$ for Cu^{1+}, $A_{ag} = 2$, $A_{eg} = A_{e'g} = 4$, and obtain finally

$$\begin{aligned} P_{440} &= -1{\cdot}47x^2/(1+x^2) \\ P_{20} &= -1{\cdot}10(x^2 - hx)/(1+x^2). \end{aligned} \qquad (8)$$

Table 3 shows that the *only* fairly model-independent quantity is the hexadecapole population P_{440}, and in particular its negative sign predicted by (8). The hybridization parameter obtained from P_{440} is of the order of $|x| \approx 0{\cdot}7$ (2) in good agreement with the value of $-\frac{1}{2}$ of Nagel (1985). The sign of x cannot be determined from the gross population P_{20}, nor probably from the deformation functions of Cu alone. Indeed, Fig. 3 indicates that h might be zero, and then $P_{440}/P_{20} = +1{\cdot}34$, which is compatible with the *.G.* refinements (anharmonic displacements). Thus, the orbital-product analysis shows numerically the invariant feature of Figs. 2(*a*)-2(*d*), *viz* the density deficiency corresponding to a partially unoccupied $3d_{z^2}$ orbital. As mentioned above, $A_{eg,e'g} = 0$ if the bond has cylindrical symmetry, and therefore $P_{443+} = 0$. This is the case for the *.G.* refinements.

The calculations were carried out at the computer center of the Swiss Federal Institute of Technology at Lausanne (CDC CYBER 170-855). The project is supported by the Swiss National Science Foundation, grants 2.067-0.81 and 2.270-0.84.

References

ATKINS, P. W. (1983). *Molecular Quantum Mechanics*, 2nd ed., pp. 72, 235. Oxford Univ. Press.

BECKER, P. J. & COPPENS, P. (1974). *Acta Cryst.* **A30**, 129-147.

BECKER, P. J. & COPPENS, P. (1975). *Acta Cryst.* **A31**, 417-425.

BLESSING, R. H., COPPENS, P. & BECKER, P. J. (1972). *J. Appl. Cryst.* **7**, 488-492.

COPPENS, P., GURU ROW, T. N., LEUNG, P., STEVENS, E. D., BECKER, P. J. & YANG, Y. W. (1979). *Acta Cryst.* **A35**, 63-72.

EICHHORN, K., SPILKER, J. & FISCHER, K. (1984). *Acta Cryst.* **A40**, C-160.

FLACK, H. D. & VINCENT, M. G. (1978). *Acta Cryst.* **A34**, 489-491.

HAFNER, S. S. & NAGEL, S. (1983). *Phys. Chem. Miner.* **9**, 19-22.

HALLBERG, J. & HANSON, R. C. (1970). *Phys. Status Solidi*, **42**, 305-310.

Handbook of Chemistry and Physics (1980). E70-E72. Cleveland, Ohio: Chemical Rubber Company.

HIRSHFELD, F. L. (1977). *Isr. J. Chem.* **16**, 226-229.

HOLLADAY, A., LEUNG, P. & COPPENS, P. (1983). *Acta Cryst.* **A39**, 377-387.

International Tables for X-ray Crystallography (1974). Vol. IV. Birmingham: Kynoch Press.

JOHNSON, C. K. & LEVY, H. A. (1974). *International Tables for X-ray Crystallography*, Vol. IV, pp. 314-319. Birmingham: Kynoch Press. (Present distributor D. Reidel, Dordrecht.)

KRÜGER, H. & MEYER-BERKHOUT, U. (1952). *Z. Phys.* **132**, 171-178.

KURKI-SUONIO, K. (1977). *Isr. J. Chem.* **16**, 115-123.

LEWIS, J., SCHWARZENBACH, D. & FLACK, H. D. (1982). *Acta Cryst.* **A38**, 733-739.

MARKSTEINER, P., BLAHA, P. & SCHWARZ, K. (1986). *Z. Phys. B.* Submitted.

MULLEN, D. & FISCHER, K. (1981). *Z. Kristallogr.* **156**, 85-86.

NAGEL, S. (1985). *J. Phys. Chem. Solids*, **46**, 743-756.

ORGEL, L. E. (1958). *J. Chem. Soc.* pp. 4186-4190.

SCHWARZENBACH, D. & NGO THONG (1979). *Acta Cryst.* **A35**, 652-658.

STEVENS, E. D. (1974). *Acta Cryst.* **A30**, 184-189.

STEWART, R. F. (1976). *Acta Cryst.* **A32**, 565-574.

WAL, H. R. VAN DER, DE BOER, J. L. & VOS, A. (1979). *Acta Cryst.* **A35**, 685-688.

WELLS, A. F. (1975). *Structural Inorganic Chemistry*, 4th ed., p. 107. Oxford: Clarendon Press.

XRAY system (1972). Tech. Rep. TR-192. Computer Science Center, Univ. of Maryland, College Park, Maryland.